

Cellulose Nano Crystals Loaded Poly (Vinyl Alcohol) Films with Enhanced Mechanical and Water Absorption Properties

Abstract

In the proposed work, poly(vinyl alcohol) films have been prepared in the presence of cellulose nano crystals to yield films with enhanced stability in aqueous medium and fair tensile strength. Cellulose nano crystals were obtained by continuous ultra-sonication of cellulose powder in water. The nano crystals had dimensions of 50 to 100 nm. The CNC loaded films were characterized by XRD, SEM, FTIR and DLS analysis. The water absorption behavior of films was studied in the physiological fluid (PF) of pH 7.4. The films, loaded with 12, 24 and 30 wt % of CNC exhibited swelling ratio (SR) of 0.80, 1.33 and 0.96 g/g respectively, thus showing unusual trend. The kinetic water uptake data were analyzed by Power function model which revealed that the water transport mechanism was less-diffusion controlled. In addition the Schott model was found to fit well and the parameters evaluated were quite close to the experimental data.

J. M. Keller

Lecturer,
Deptt.of Physics,
University Teaching Department,
Rani Durgawati Vishwavidyalaya,
Jabalpur, M.P.

Keywords: Hydrogel Films, Cross-Linking, Water Uptake Analysis, Less-Fickian Swelling, Physiological Fluid (PF).

Introduction

Polymer Science is one of the most promising branch of modern science, because of widespread applications of polymers all over the world in almost all fields such as construction, communication, medical science, textile, transport, space and technology etc. Poly(vinyl alcohol) is a biocompatible and biodegradable polymer, usually obtained by hydrolysis of poly(vinyl acetate) [1]. The concept of eco-friendly chemistry and concerns for the safety of the environment have motivated chemists and nonscientists to look for green chemistry based methods to prepare nanoparticles [2-3] toxicity of coinage metal nanoparticles has been the key cause for their constant use in various biomedical applications [4-5]. PVA has been widely employed in a large number of biomedical applications due to its biodegradable and biocompatible nature. These applications include drug delivery *in vitro* [6-9], tissue engineering [10], wound dressings [11], porous scaffolds [12] etc. In addition, PVA is also used for food packaging [13]. The wound dressing usually consists of a natural or synthetic polymer matrix that is adequate of consumption of exudates with concurrent clemency of the meshed bioactive agent at a pre-determined rate. A huge number of wound dressings, comprising of both natural as well as synthetic polymers, have been reported in recent past [14-16]. In spite of having excellent film forming property, mechanical strength and water absorption behavior, PVA films suffer from a major drawback that they have a very strong dissolution tendency in aqueous medium. This restricts its use for applications such as drug delivery and wound dressings where the polymers has to maintain its structural integrity in physiological fluid for a long time period while delivering the entrapped biologically active ingredients. This problem is usually overcome by carrying out chemical cross-linking of PVA with an appropriate cross-linker such as formaldehyde, glutaraldehyde, epichlorohydrin etc.[17] This is a most adopted strategy to prevent the PVA hydrogel from dissolution and has been used frequently in various biomedical applications. For example, Garnica-Palafox et al.[18] have investigated mechanical properties of PVA/chitosan hydrogels cross-linked with epichlorohydrin. In another work, Kumar and co-worker[19] have produced PVA, sodium alginate and chitosan based hydrogels cross-linked by glyoxal. The films were

Nema Mishra

Research Scholar,
Deptt.of Physics,
University Teaching Department,
Rani Durgawati Vishwavidyalaya,
Jabalpur, M.P.

characterized by various analytical techniques. In order to avoid using toxic cross-linking agents, attempts have been made to modify PVA using non-toxic chemicals. For example, most recently, Zhang et al.[20] have modified PVA by grafting it with succinate acid to yield carboxyl-modified poly(vinyl alcohol) (PVA-COOH). This was later used as a cross-linker to prepare chitosan based hydrogels via amide linkage formation. In another strategy, H-bonding interactions have been employed as physical cross-links to prevent PVA based hydrogels from dissolution. Most recently, Tian et al.[21] have prepared PVA/starch blends by melt process and reported their physico-chemical properties. The H-bonding interactions between starch and PVA affected properties of blends.

In the present work, we have used cellulose nano crystals as an additive to not only strengthen the PVA films but also to prevent them from dissolution. Cellulose is the most abundantly found bio-polymer in nature and is biocompatible and biodegradable [22]. It has frequently been used in a number of biomedical applications. It is speculated that presence of a large number of hydroxyls along its backbone may bind to the -OH groups of PVA chains through H-bonding interactions to serve as additional cross-links and provide stability to PVA hydrogels.

Objective of the Study

Poly(vinyl alcohol) is a biocompatible, polymer with excellent film forming properties. However, it has to be crosslinked with toxic cross-linkers like glutaraldehyde, formaldehyde etc. in order to prevent the films against dissolution. In this work, for first time we have produced insoluble films by loading cellulose nanocrystals into PVA films without using any toxic chemical. The CNC were prepared by physical method, i.e. ultra sonication of cellulose suspension in water. Their mechanical and water absorption properties were also studied.

Materials, Methods and Equipment's

Poly (vinyl alcohol), cellulose powder were purchased from Mi Media, Mumbai and used as received. CNC were obtained by continuous ultra-sonication of cellulose suspension for 5 days. The CNC were characterized by DLS, XRD, TGA, SEM, AFM analysis. The films were produced by solvent evaporation method which involves dissolution of PVA in water, followed by addition of CNC under stirring and evaporation of water to get films. Films were tested for mechanical and water absorption properties.

The cellulose nano crystals (CNC) were found to have nano sized particle size in the range of 50 to 90 nm. The DLS analysis also confirmed this finding. In addition, TEM analysis supported this finding. The CNC loaded films were found to be insoluble in water even three days after immersion in water. The water uptake was found to decrease with increase in the cellulose contents. The CNC/PVA films showed excellent mechanical properties, which increased with cellulose contents. The results were explained by the presence of H-bonding interactions between hydroxyls of cellulose and PVA. The control PVA films were found to dissolve in a few h after

immersion. In this way this is an excellent way to produce PVA films with fair mechanical strength and water absorption.

Review of Literature

A review on polymeric hydrogel membranes for wound dressing applications: PVA-based hydrogel dressings. Kamoun EA, Kenawy ES, Chen X. *J Adv Res.* 2017 May;8(3):217-233. *J Biomater Sci Polym Ed.* 2017 May;28(7):664-678. Collagen-PVA aligned nanofiber on collagen sponge as bi-layered scaffold for surface cartilage repair. Lin H.Y, Tsai WC2, Chang S.H. Preparation and Application of Starch/Polyvinyl Alcohol/Citric Acid Ternary Blend Antimicrobial Functional Food Packaging Films ZhijunWu, Jingjing Wu, TingtingPeng 2, Yutong Li 2, Derong Lin 2,*, Baoshan Xing 3,*, Chunxiao Li 2, Yuqiu Yang 2, Li Yang 2, Lihua Zhang 1, Rongchao Ma 1, Weixiong Wu 1, XiaorongLv 2, Jianwu Dai 2 and Guoquan Han, *Polymers* 2017, 9,102-121

Experimental

Materials

Poly (vinyl alcohol) (PVA; degree of substitution 95 %), cellulose powder (Cell), and other chemicals were purchased from Hi Media Chemicals, Mumbai, India. The double distilled water was used throughout the investigations.

Preparation of CNC/PVA composite films

The CNC/PVA composite films were prepared by solvent evaporation method. In brief, 10 % (wt/vol) PVA solution of PVA was prepared in distilled water. Now, definite volumes of the above prepared CNC suspension and PVA solution were mixed under moderate stirring to give a total volume of 50 mL. The solutions were poured into Petri plates and put in electric oven (Temp star, India) at 60°C for a period of 4 h. The films, so prepared, were peeled off carefully and placed in a dust free chamber for further use. In all four samples were prepared, designated as CNC/PVA(x), where x is the wt % of CNC in the film with respect to PVA content. The films shall be designated as CNC/PVA (0), CNC/PVA(12), CNC/PVA(18) and CNC/PVA(24).

Characterization of films

The Fourier Transform Infrared (FTIR) spectra were recorded with an FTIR spectrophotometer (Shimadzu, 8400, Japan) using KBr. The powdered sample was mixed with KBr. The scans recorded were the average of 100 scans and the selected spectral range between 400 to 4000 cm^{-1} .

The X-ray diffraction (XRD) method was used to measure the crystalline nature of the films. These measurements were carried out on a Rigaku Diffractometer (Cu radiation = 0.1546 nm) running at 40 kV and 40 mA. The diffractogram was recorded in the range of 2 from 3 to 50° at the speed rate of 2 degree/ min.

Nanocellulose particle size analysis was conducted by dynamic light scattering (DLS) using a Zeta seizer NanoZS instrument (Malvern, UK),

In order to investigate the surface morphology of films, SEM images were recorded at IISER, Pune (Maharashtra State), India.

Swelling Studies

Swelling studies were carried out in the pseudo extracellular fluid (PEF) as described by Lin et al. [23]. This simulated wound fluid has following composition : 2.2 g of KCl, 6.8 g of NaCl, 25 g of sodium bicarbonate and 3.5 g of sodium di-hydrogen phosphate in 1 liter. The pH of this solution was found 7.36. The pre-weighed film sample was placed in 100 mL of PEF at 37°C and it was taken out at different time intervals, wiped superficially with tissue paper to remove extra surface water, weighed accurately in an electronic balance (Denber, Germany), and then placed back in water. The swelling Ratio(SR) determined at different time intervals using the following expression:

$$SR = \frac{(m_t - m_0)}{m_0} \text{ g/g} \quad \dots (1)$$

Where m_0 and m_t are the initial mass and mass at different time intervals respectively. In order to determine Equilibrium Swelling Ratio (ESR), m_t was replaced by m_e which is the weight of the swollen film at equilibrium.

Results and discussion**Preparation of cellulose nano crystals**

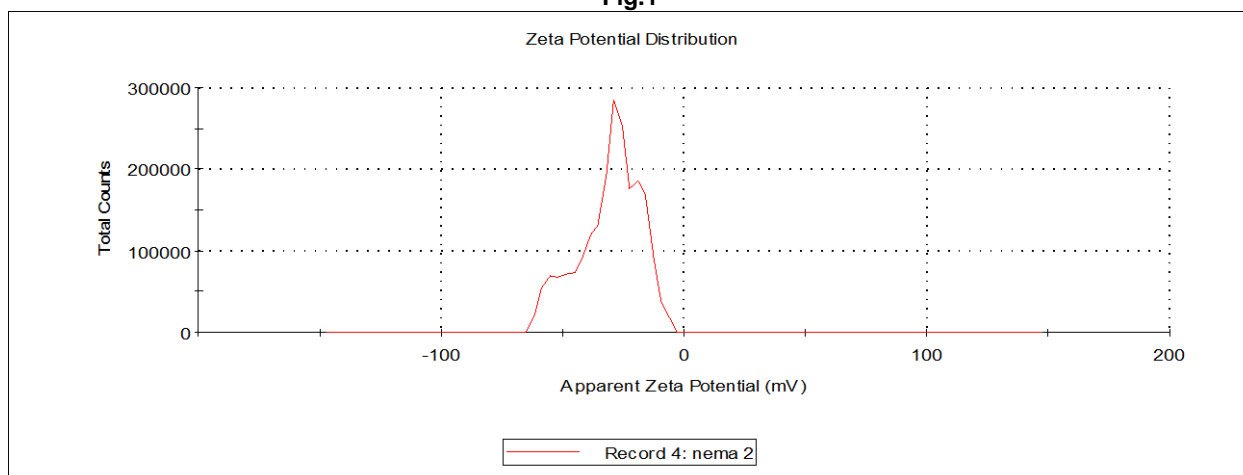
In this work, cellulose particles were ultrasonicated for total period of 5 days, with an exposure frequency of 5 h per day which enabled us to obtain cellulose nano crystals. The ultrasonic waves penetrate through the amorphous region of cellulose chains and break them in to smaller sized chains with dimension in the nano scale range.

Preparation of CNC/PVA films

In the present work, Cellulose nano crystals have been well dispersed in to PVA film matrix. The film forming solution consists of well dispersed CNCs in the aqueous solution of PVA. When the solution is poured in to Petri plates and the solvent is evaporated, the CNC/PVA film is produced. Here, it may be considered that -OH groups along the PVA chains may act as templates to bind with cellulose nano crystals through H-bonding interactions. After the solvent is evaporated, a uniformly distributed array of cellulose nano crystals is obtained within the film.

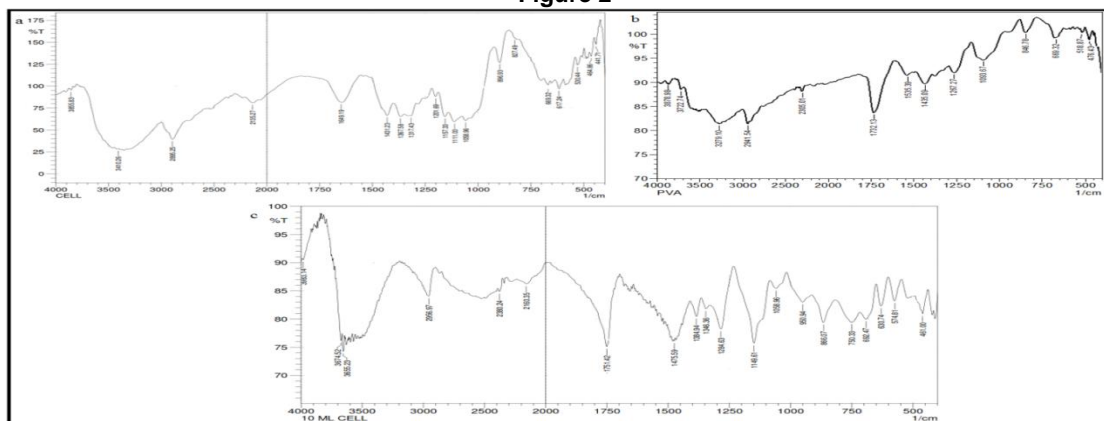
Characterization of films

Dynamic light scattering (DLS) analysis was also employed to find the statistical distribution of the nanocellulose particles present in the dispersion. zeta potential = -30.6 mV Mobility = -2.397 $\mu\text{m cm/Vs}$ conductivity = 0.0568 mS/cm

Fig.1

The FTIR spectra of pure cellulose, native PVA and CNC/PVA(18) film are shown in Fig. 2(a) (b) and (c) respectively. It can be observed in Fig. 2(a) that there is a strong broad band at around 3410 cm^{-1} , which is assigned to different O-H stretching

modes. The characteristic peak at 2896 cm^{-1} shows C-H, CH_2 stretching of cellulose. The bands at 1367, 1201, 1157 and 1058 cm^{-1} are assigned to C=O, C-H, C-O-C and C-O deformation or stretching vibrations of different groups in carbohydrates [24].

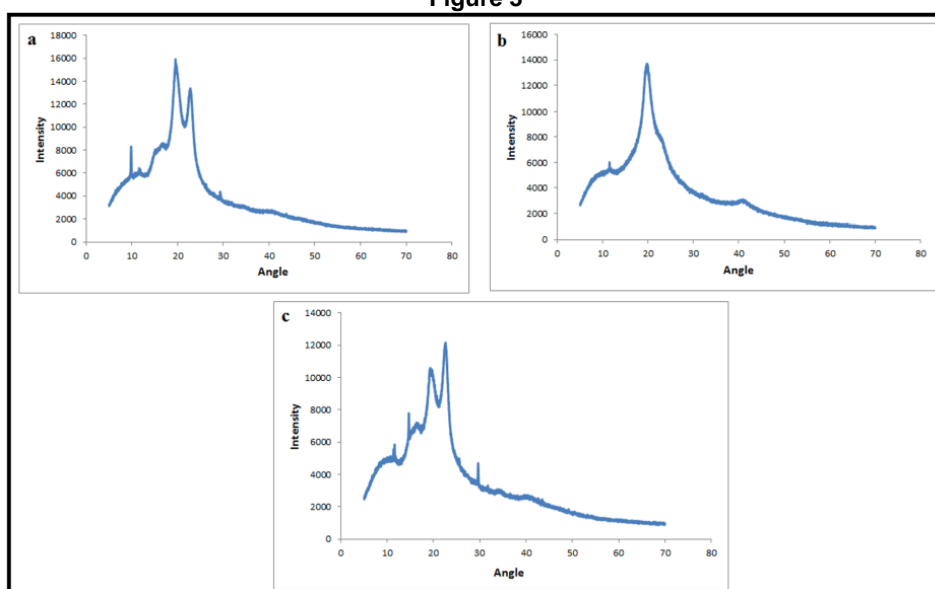
Figure 2

Finally, absorption band at 897 cm^{-1} is assigned to $-\text{C}-\text{O}-\text{C}$ stretching at β -(1 \rightarrow 4) glycosidic linkage[25]. In the spectrum of PVA, as shown in Fig.2 (b), the 3279 cm^{-1} and 2941 cm^{-1} are the $-\text{OH}$ and CH_2 stretching vibrations. The $\text{C}-\text{O}$ stretching range is at 1093 cm^{-1} . The spectrum of composite film, displayed in Fig.2 (c) reveals that $\text{C}-\text{H}$ alkyl stretching band appears at 2956 cm^{-1} ($\nu = 2850-3000 \text{ cm}^{-1}$), superimposing the sharp peak obtained due to $\text{C}-\text{H}$, CH_2 stretching of native cellulose. It is also noticed that typical strong hydroxyl bands for free alcohol (non-bonded $-\text{OH}$ stretching band at $\nu = 3600-3650 \text{ cm}^{-1}$), and hydrogen bonded band ($\nu = 3200-3570 \text{ cm}^{-1}$) also appear in the spectrum of composite film.

In addition, the $\text{C}-\text{O}$ stretching, a characteristic peak for PVA, appears at approximately

1111 cm^{-1} . The diffraction pattern of native cellulose, shown in Fig.3(a), confirm relatively suppressed peak at $2\theta = 14.62^\circ(1\bar{1}0)$ and a sharp peak at $22.48^\circ(200)$, thus indicating the presence of cellulose I.[26]. In addition a sharp peak also appears at $2\theta = 21.53^\circ(200)$, indicating presence of cellulose II structure[27]. The XRD pattern of the pure PVA film, as shown in Fig.3(b) indicates strong crystalline reflections at around $2\theta = 19.92^\circ$ and a shoulder at 22.74° . The two peaks are characteristic of PVA, representing reflections from (101) and (200) from a monoclinic unit cell [28]. Finally, the XRD pattern of CNC/PVA(18), displayed in Fig.3(c) indicates presence of nearly all the peaks that exist in diffractogram of cellulose and PVA as mentioned above.

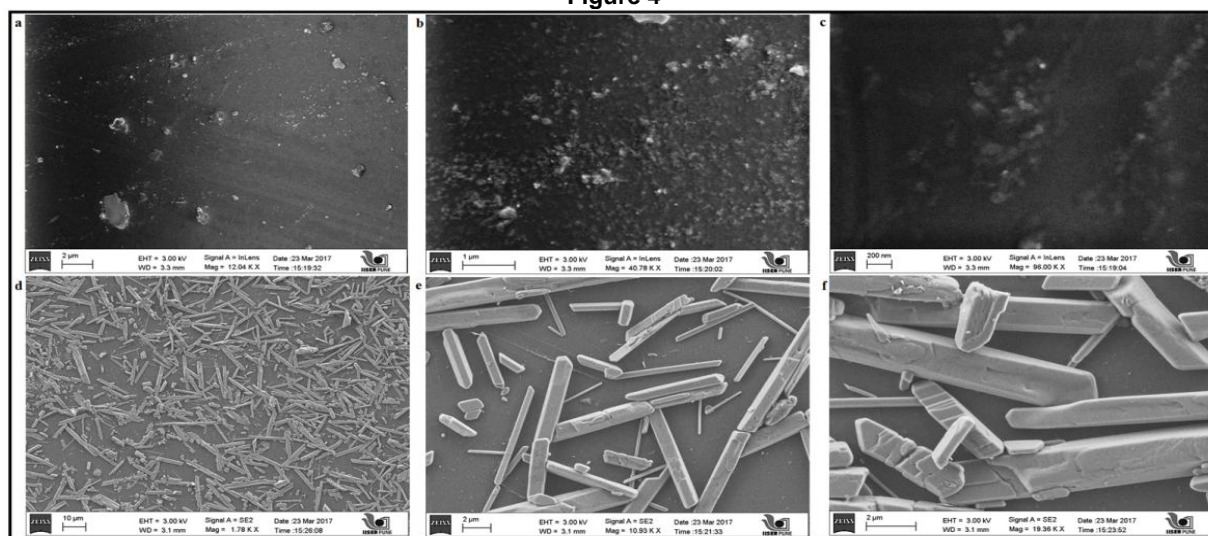
Figure 3



The Scanning electron microscopy (SEM) was carried out to investigate surface texture of the plain and CNC loaded films. The results for the plain CMC/PVA(0) are shown in Fig.4(a-c) with magnifications of 12000, 40000 and 96000

respectively. The surface texture, shown in Fig.2(a) indicates a little rough surface with a little agglomeration at some places, probably due to the presence of some impurities or un-dissolved PVA crystals.

Figure 4



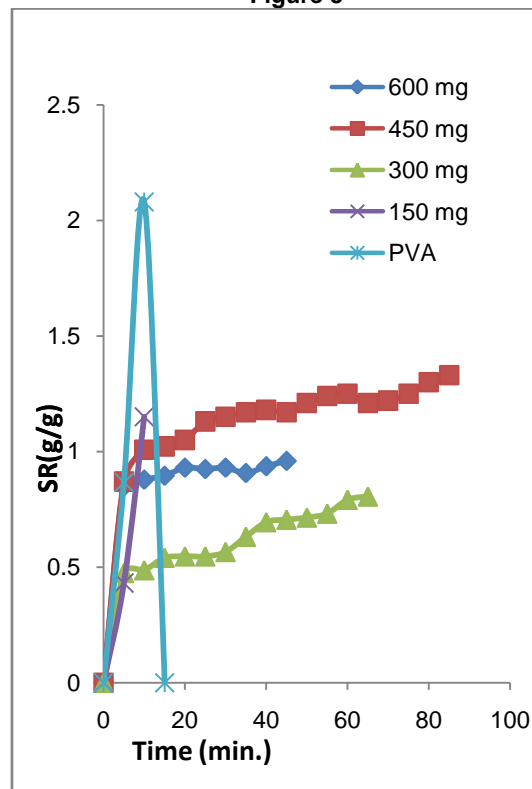
The Fig. 4(b) also supports this observation. Finally, the image, displayed in Fig.4(c) reveals that the particulates are up to 500 nm .The SEM images of sample CNC/PVA(18) are displayed in Fig.4(d-f) with relative magnifications of 1780, 10930 and 19360 X respectively. It can be observed in Fig.4 (d) that the cellulose crystals are almost uniformly distributed throughout the film matrix, though at some places the density is not so high as compared to other places.A further observation at still higher magnifications, displayed in Fig.4(e-f) reveal that cellulose crystals have bar-like geometry and some crystals quite differ in size and dimensions.

Swelling Behavior

The water absorption behavior of plain PVA and CNC/PVA films containing different cellulose contents were studied in the phosphate buffer saline(PBS) of medium 7.4 The results are shown in Fig.5,6. It can be seen that the plain PVA film shows a faster swelling and attains ESR of 2.1 in 15 min. However, thereafter it begins to lose weight and dissolves completely in next 5 min. On the other hand, the film samples CAN/PVA (12), CNC/PVA(18) and CNC/PVA(24) show total swelling ratios of 0.80, 1.33 and 0.95 g/g respectively. It took almost 45 to 80 min for the samples to attain equilibrium swelling ratio (ESR).

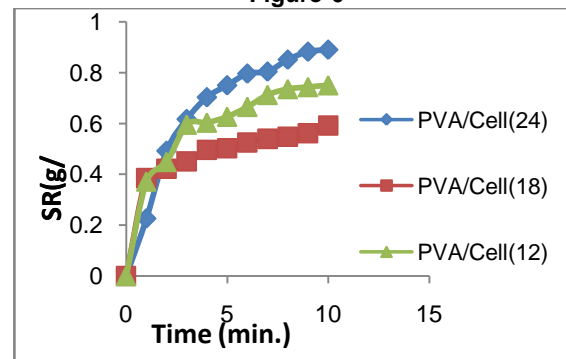
TIME	% SWELLING				
	600 mg	450 mg	300 mg	150 mg	PVA
0	0	0	0	0	0
5	0.849	0.87	0.475	0.431	0.867
10	0.878	1.008	0.487	1.15	2.08
15	0.895	1.022	0.541		0
20	0.93	1.05	0.547		
25	0.924	1.13	0.547		
30	0.93	1.15	0.566		
35	0.907	1.17	0.632		
40	0.936	1.18	0.695		
45	0.959	1.17	0.706		
50		1.21	0.715		
55		1.24	0.732		
60		1.25	0.792		
65		1.21	0.806		
70		1.22			
75		1.25			
80		1.3			
85		1.33			
M _{inf}	0.959	1.33	0.806	1.15	2.08

Overall swelling (Final)
Figure 5



Time (min.)	PVA/Cell (24)	PVA/Cell (18)	PVA/Cell (12)
0	0	0	0
1	0.226	0.385	0.372
2	0.492	0.422	0.449
3	0.617	0.451	0.596
4	0.703	0.496	0.604
5	0.75	0.503	0.627
6	0.796	0.525	0.666
7	0.804	0.54	0.713
8	0.851	0.548	0.736
9	0.882	0.562	0.744
10	0.89	0.592	0.751

Figure-6

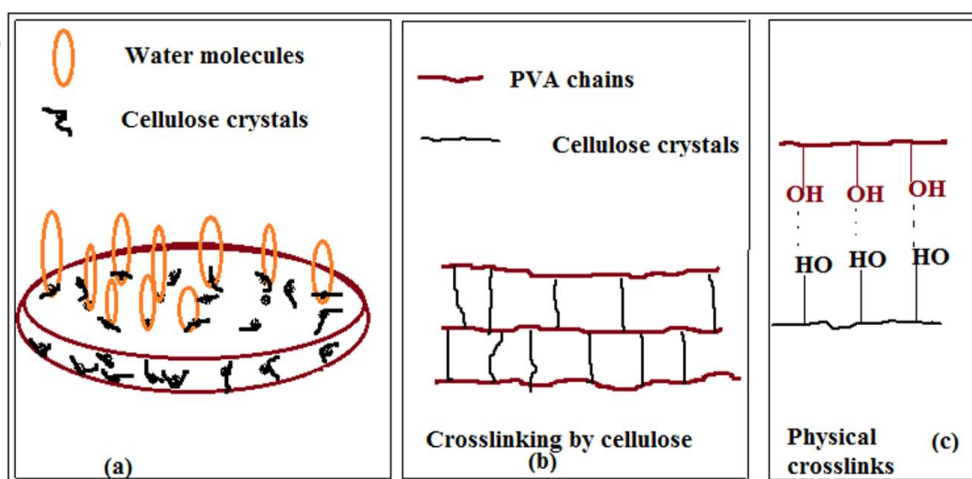


Early stage kinetics (final)

The observed swelling data for the film samples CAN/PVA (12), CNC/PVA(18) and CNC/PVA(24) suggest that as the cellulose content in the film increases from 12 to 18 % (w/v), the ESR also increases. However, with the further increase in the cellulose content to 24 %(w/v),the ESR begins to decrease. The results may be explained as follows. Initially, the increase in CNC content from 12 to 18 % causes an increase in the surface hydroxyls due to presence of cellulose. These –OH groups interact with incoming water molecules and bind to them, thus resulting in higher water uptake. In addition, the added cellulose crystals also impart stability to the film by establishing physical cross-links with the –OH groups of PVA chains. However, as the cellulose content is further increased from 18 to 24 wt %, the cellulose crystals produce, present within the bulk of

the film matrix, and produce more physical cross-links through H-bonding interactions with hydroxyls of PVA chains. These physical cross-links result in a decrease in the free space available for accommodation of incoming water molecules. In addition relaxation of PVA chains is also restricted due to increased cross-linking. It is also noteworthy that all the three samples, containing cellulose within the film matrix, show enhanced stability for more than 72 h, while the pure PVA film just dissolves in 15 min. Therefore it may be concluded that addition of cellulose nanocrystals in to the PVA film matrix, causes the films to be highly stable in aqueous medium. The schematic illustration of interactions of cellulose molecules with PVA chains within the film samples CAN/PVA(12), CNC/PVA(18) and CNC/PVA(24) is shown in Fig.7.

Figure 7



It may be observed in Fig.7 (a) that water molecules, entering in to the film matrix are attached to the surface hydroxyls of cellulosic micrometer sized crystals, thus enhancing the water absorption behavior. However, as the cellulose content increases, the cellulose microcrystals produce additional cross-links (see Fig.7 (b)). These physical cross-links are well illustrated in Fig.7(c).

Modeling of the water uptake data

The water penetration mechanism of the CNC/PVA films was best investigated using the well-

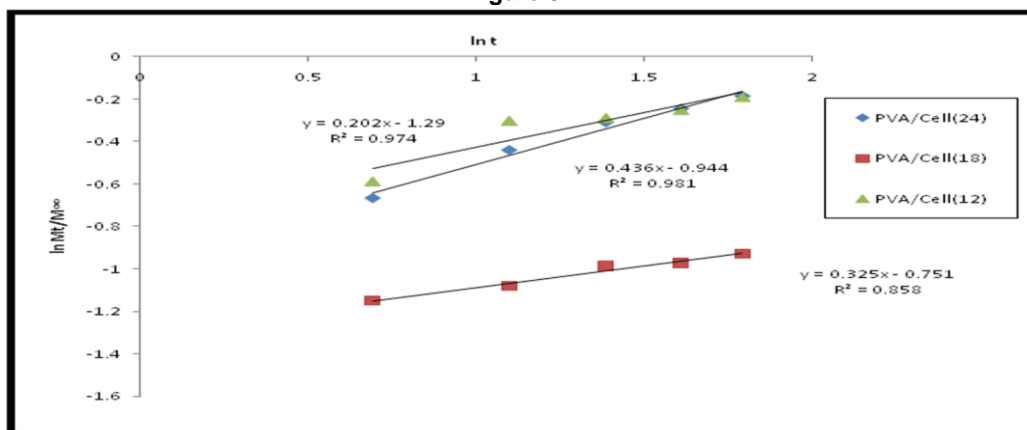
known “Power function model”, developed by Peppas [29]. According to this model

$$\frac{M_t}{M_\infty} = k t^n \dots (2)$$

Where M_t and M_∞ are the masses of the hydrated film sample at time ‘t’ and at equilibrium respectively; ‘n’ and ‘k’ are the swelling exponent and gel-characteristic constants respectively. The logarithmic form of the above equation may be written as

$$\ln \frac{M_t}{M_\infty} = \ln k + n \ln t \dots (3)$$

Figure 8



The initial 60% water uptake data was used to draw linear plots between $\ln M_t / M_\infty$ and $\ln t$, which yielded straight lines with fairly higher regressions., as shown in Fig.8. It was observed that the swelling exponent 'n' for the samples CAN/PVA (12), CNC/PVA(18) and CNC/PVA(24) was found to be 0.20, 0.32 and 0.41 respectively. These values are quite below than 0.5, thus suggesting 'less Fickian' behavior of the films. This indicates that for all the three film samples, rate of diffusion of water into hydrogel films is much smaller than the rate of relaxation of polymeric chains. This may be explained on the basis of the facts that poly (vinyl alcohol) chains undergo faster relaxation due to strong interactions with incoming water molecules. But the diffusion of water into the matrix takes place at very slow rate due to presence of cellulose crystals which act as diffusion barrier for the incoming water molecules. Almost similar results were also reported in our previous work for the swelling behavior of PVA/Carrageenan cross-linked hydrogel films [30].

All the related parameters for the three film samples are given in Table -1

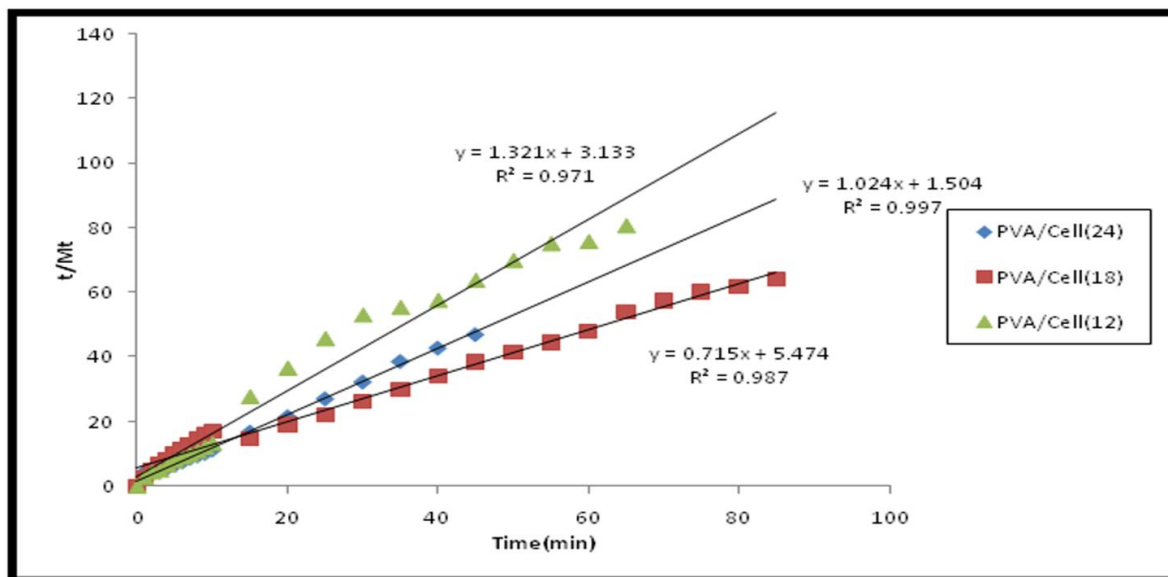
Table 1
Values of Various Parameters Associated With Kinetics Models

Sample code	$M_\infty(\text{theor})$ (g/g)	K_2	$\gamma_{\text{in(theor)}}$	$M_\infty(\text{exp})$ (g/g)	R^2
PVA/Cell(12)	0.7567	0.55715	0.3191	0.806	0.9719
PVA/Cell(18)	1.3976	0.09352	1.8267	1.33	0.9879
PVA/Cell(24)	0.9758	0.69809	0.66484	0.959	0.9975

The Schott kinetic model was also applied on the kinetic water absorption data. According to this model [31]:

$$dM_t/dt = k_2 (M_\infty - M_t)^2 \dots (4)$$

Figure 9



Where, M_t is the water uptake at time 't' and ' k_2 ' is the second order rate constant for water absorption process. On integrating above equation within the limits $t=0, M_t=0$ and $t=\infty, M_t=M_\infty$, following equation is obtained:

$$t/M_t = 1/k_2 M_\infty^2 + t/M_\infty$$

Or

$$t/M_t = A + B t \dots (5)$$

Where, A and B are two coefficients whose physical meaning is interpreted as follows: At a long retention time $Bt \gg A$ and therefore $B = 1/M_\infty$, that is, B is reciprocal of the maximum water uptake. On the contrast, at a very short time interval $Bt \ll A$ and so, $Lt (dM_t/dt) = 1/A$... (6)

$t \rightarrow 0$

Therefore, the intercept A is reciprocal of initial swelling rate. In order to apply this model, the kinetic data were used to draw plots between t/M_t and t as shown in Fig.9. The slopes and intercepts of linear plots were employed to evaluate the rate

constant k, equilibrium water uptake M_∞ and initial swelling rate (i.e. $r_{ini} = 1/A$). All these parameters are shown in Table-I. A close look at the various parameters, obtained for the Schott model, reveals that for all the samples regressions are fairly high thus indicating the suitability of the Schott model. In addition, it may also be noticed that the theoretical and experimental SR values are quite close to each other, thus further confirming the validity of this model.

Conclusion

It may be concluded from the above study that entrapment of cellulose microcrystals in to un-cross-linked poly(vinyl alcohol) film renders it with fair stability in the physiological fluid while the un-cross-linked film dissolves within 20 min after its immersion. In addition, the water absorption behavior of CMC-reinforced PVA films follows Fickian water transport mechanism. Since the PVA films have been stabilized through entrapment of cellulose micro-crystals, and no toxic chemical has been used throughout the

study, these films have great potential to be used for biomedical applications.

Acknowledgement

It's my great privilege to. Pay sincere thanks to Dr.S.K.Bajpai and Dr.Manjula Bajpai.

References

1. Kamoun, E. A., Kenawy, E. S., Chen, X., (2017) PVA-based hydrogel dressings, *J Adv Res.* 8(3):217-233.
2. Sadeghi, B., Gholamhoseinpoor, F. (2015) *Acta A Mol Biomol Spectrosc.* 134:310-5.
3. Hu, Y., Wu, B., Jin, Q., Wang, X., Li, Y., Sun, Y., Huo, J., Zhao, X, Facile. (2016) *Talanta* 152:504-12.
4. Amedea, B., Seabra, Nelson D. (2015) *Nanotoxicology of Metal Oxide Nanoparticles Metals* 5, 934-975.
5. Avinash, P., Ingle Nelson Duran. (2014) *Applied Microbiology and Biotechnology* 98: 1001–1009.
6. Martínez-Gómez, F., Guerrero, J., Matsuhiro, B., Pavez, J., (2017) *Carbohydr Polym.* 155:182-191
7. Abdelkader, D. H., Osman, M.A., El-Gizawy, S. A., Faheem, A. M., McCarron, P.A., (2016) *Int J Pharm.* 500(1-2):326-35.
8. Jensen, B.E., Davila, I., Zelikin, A.N., *Phys Chem, B.* J., (2016) 120(26):5916-26.
9. Heaysman, C.L., Phillips, G.J., Lloyd, A.W., Lewis, A.L., (2016) *J Mater Sci Mater Med.* 27(3):53.
10. Kumar, A., Han, S. S., (2017) *International Journal Of Polymeric Materials And Polymeric Biomaterials.* 66: 159-182.
11. Kamoun, E.A., Kenawy, E.S., Chen, X., (2017) *J Adv Res.* 8(3): 217-233.
12. Lin, H.Y., Tsai, W.C., Chang, S.H., etc. (2017) *J Biomater Sci Polym Ed.* 28(7):664-678.
13. Wu, Z., Wu, J., Peng, T., Li, Y., Lin, D., Xing, B., Li, C., Yang, Y., Yang, L., Zhang, L., Ma, R., Wu, W., Lv, X., Dai, J., Han, G., (2017) 102-121.
14. Fu, L., Zhou, P., Zhang, S., Yang, G. (2013) *Material Sci. Eng. C Mater. Biol. Appl.*, 33(5), 2995-3000
15. Liakos, I., Rizzello, L., Bayer, I.S. Pompa, P. P., Cingolani, R., Athanassiou, A. (2013) *Carbohydrate Polym.* 92(1): 176-183
16. Shojaee-Aliabadi, S., Hosseini, H., Mohammadifar, M.A., Mohammadi, A., Ghasemlou, M., Hosseini, S.M., Khaksar, R. (2014) *Carbohydr. Polym.* 101, 582-91.
17. Kamouna, E.A., Chenb, X., Mohy Eldina, M. S., Kenawy, E. S., (2015) *Arabian Journal of Chemistry* 8(1): 1–14.
18. Garnica-Palafox, I. M., Sánchez-Arevalo, F.M., Velasquillo, C., García-Carvajal, Z. Y., García-Lopez, J., Ortega-Sánchez, C., Ibarra, C., Luna-Barcenas, G., Solís-Arrieta, L., (2014) *J Biomater Sci Polym Ed.* 25(1):32-50,
19. Kumar, A., (2017) *Mater Sci Eng C Mater Biol Appl.* 73:333-339
20. Zhang, D., Zhou, W., Wei, B., Wang, X., Tang, R., Nie, J., Wang, J., (2015) *Carbohydr Polym.* 125: 189-99.
21. Ruth, S.M., Poblete, S., Joy, L., Diaz, L., (2014) *Advanced Materials Research,* 925:379-384 .
22. Tang, L., Huang, B., Wang, Q. U.S., Oua, W., Lina, W., Chena, X., (2013) *Bioresource Technology Volume* 127:100–105
23. Lin, S. Y., Chen, K. S., Run-Chu, L., (2001) *Biomaterials* 22: 2999.
24. Poletto, M., Ornaghi, H. L. Jr., Zattera, A. J., (2014) 7 :6105-6119.
25. Kondo, T., (1997) *The assignment of IR absorption bands due to free hydroxyl groups in cellulose.* 4:281–292.
26. Ciolacu, D., Ciolacu, F., Popa, Y. I., (2011) 45(1-2):13-21.
27. Kumar, A., Negi, Y.S., Bhardwaj, N. K., Choudhary, V., (2013) *Adv. Mat. Lett.* 4 (8):626-631.
28. Johar, N., Ahmada, I., Dufresne, A., (2012) *Indus. Crop. Prod.* 37:93-99.
29. Tang, C. M., Tian, Y. H., Hsu, S. H., (2015) 8: 4895-4911.
30. Peppas, N. A., Kormsmeier, R. W., Boca Raton CRC Press (1986) 27-56.
31. Drużyńska, M. G., Czubenko, J. O., (2012) 17:59-66.
32. Schott, H., (1992) *J. Macromol. Sci. Part B.* 31: 1–9.
33. Dussán, K. J., Silva, D. D. V., Moraes, E. J. C., Arruda, P. V., Felipe, M. G. A., (2014) 38:433-438.
34. Saito, T., Nishiyama, Y., Putaux, J. L., Vignon, M., Isogai, A., (2006) *Biomacromolecules,* 7 (6):1687-1691.
35. Cuia, S., Zhanga, B. S., Gea, S., Xionga, L., Suna, Q., (2016) 83:346–352.
36. Tian, H., Yan, J., Rajulu, A.V., Xiang, A., Luo, X., (2017) *Int J Biol Macromol.* 96:518-523